3P1-18

Proceedings of Symposium on Ultrasonic Electronics, Vol. 30 (2009) pp. 457-458
18-20 November, 2009

Time-resolved imaging of confined Rayleigh and Lamb waves in microscopic resonators and wedges

マイクロ共振器・くさび構造中のレイリー波・ラム波の時間分解イメージング

Motonobu Tomoda[1†], Shinnosuke Matsueda[1], Oliver B. Wright[1], Osamu Matsuda[1], Yoshiaki Nishijima[2], Kosei Ueno[2], Juodkazis Saulius[2], and Hiroaki Misawa[2]
([1]Grad. Sch. Eng., Hokkaido Univ.; [2]RIES, Hokkaido Univ.)
友田基信 [1†], 松枝真之介 [1], Oliver B. Wright[1], 松田理 [1], 西島善明 [2], 上野貢生 [2], Juodkazis Saulius[2], 三澤弘明 [2] ([1] 北大 工; [2] 北大 電科研)

1. Introduction

Surface-acoustic (Rayleigh) and Lamb waves propagate along surfaces and in plates, respectively. They are important in nondestructive testing, in sensors and in filtering applications.

Here we investigate surface acoustic waves (SAWs) confined in novel resonator geometries and Lamb waves in wedge like films using an ultrafast optical technique for point thermoelastic generation and subsequent imaging [1]. In case of confined SAWs, we make use of a circular microcavity formed on a crystalline silicon substrate. We show how the resonance frequency depends on propagation direction. In the case of Lamb waves in gold wedges on a silicon nitride membrane we image the 1st order antisymmetric Lamb waves (flexural modes), and show how the sound velocity varies with wedge thickness. Sound in wedges is interesting from a theoretical standpoint because of analogies with the physics of black holes [2-3]: waves in free-standing isotropic wedges whose thickness varies quadratically with distance along the wedge are predicted not to reflect acoustic waves.

2. Imaging method

Fig. 1 shows a schematic diagram of the imaging system. The method is based on the optical pump-probe technique with a femtosecond pulsed laser. Our mode-locked Ti:Sapphire femtosecond laser system delivers ~100 fs duration optical pulses. Pump and probe pulses at wavelengths 415 nm and 830 nm, respectively, are used with a pump pulse energy, ~0.1 nJ, selected at about half of the damage threshold. The pump and probe beams are focused to ~1 μm diameter circular spots on the sample.

Each pump pulse generates Rayleigh or Lamb waves of wavelength ~10 μm at frequencies up to ~1 GHz. After passing through an optical delay line, the probe beam traverses a Sagnac interferometer that monitors changes in optical phase arising from out-of-plane surface velocity [1]. The probe spot position is scanned in two dimensions (2D) over the sample surface to form an image. Animations up to 12.4 ns (one cycle of laser repetition) can be obtained by varying the delay time between the pump and probe pulses.

The same setup can be used to generate and detect longitudinal ultrasonic pulses in the wedge samples. These waves propagate in the through-thickness direction [4]. The wedge thickness distribution can be mapped in this way by scanning the position of the sample mounted on a 2D translation stage and monitoring the time of return of these pulses to the point of excitation.

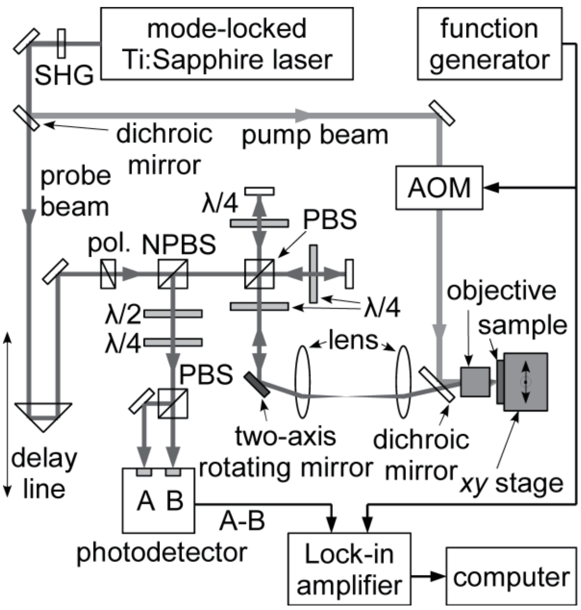

Fig. 1. Schematic diagram of the imaging system. SHG: second harmonic generation crystal, AOM: acousto-optical modulator, pol.: polarizer, NPBS: non-polarizing beam splitter, PBS: polarizing beam splitter, $\lambda/4$: quarter-wave retarder, and $\lambda/2$: half-wave retarder.

---

mtomoda@eng.hokudai.ac.jp

3. Samples

We use micro-fabrication methods including lithography and dry etching to make the SAW resonators (**Fig. 2** (a)). The samples are made on a silicon (100) wafer by plasma dry etching using a mixture of SF_6 and C_4F_8 gases. Grooves of depth and width ~10 μm are etched in the Si in the shape of circles. The sample is then coated with a polycrystalline chromium film of thickness ~40 nm to enhance the optical pump absorption and probe pulse reflection.

Polycrystalline gold wedges of various shapes are prepared by rf sputtering, making use of a programmable shutter on a translation stage inside the vacuum chamber. The substrate is a commercial polycrystalline silicon nitride membrane with a thickness of 100 nm. The thickness of the gold wedge typically changes linearly from 6 μm to zero over a length of ~200 μm.

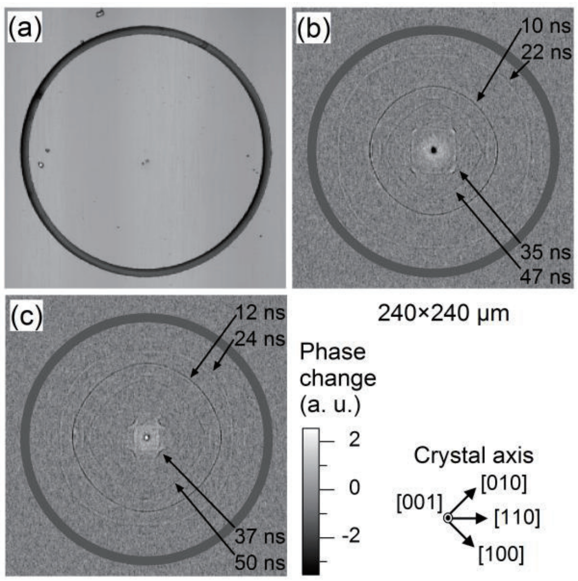

Fig. 2 (a) Optical reflectivity image of a circular Si resonator of internal diameter 200 μm. (b), (c) Snapshot of the SAW propagation. The times elapsed after the moment of pump pulse arrival are indicated by the arrows.

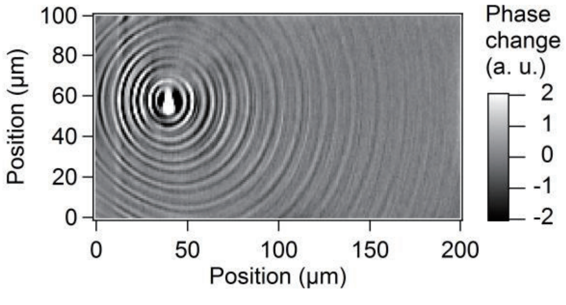

Fig. 3 Snapshot of Lamb wave propagation in a gold wedge on a SiN membrane (100 nm in thickness). The thickness of the gold wedge increases approximately linearly to the right (0 nm thickness at position 10 μm to 800 nm at 200 μm).

4. Results

SAW propagation images for the circular resonator were obtained as animations over 12.4 ns. **Figs. 2** (b) and (c) are typical images. The silicon (100) surface shows fourfold rotational symmetry in its linear elastic properties. SAWs propagating along [010] (and in equivalent symmetry directions) are Rayleigh-like modes, and SAWs propagating along [011] (and in equivalent symmetry directions) are pseudo-SAW modes [5]. This anisotropy reflects the ripple patterns in Fig. 2 (b).

Fig. 3 shows typical Lamb wave images for an approximately linear wedge using a point source. The group velocity of the ripples is seen to decrease as the thickness decreases, as is expected theoretically.

By the use of temporal Fourier analysis, we obtain spectral amplitude and phase images at constant frequencies, and also dispersion relations by a further 2D spatial Fourier transform. In particular, for the resonator results, this process reveals resonant frequencies that depend on propagation direction.

5. Conclusions

We have imaged the propagation of surface-acoustic and Lamb waves on circular resonators and in metal wedges respectively. Further work of interest involves increasing the ultrasonic energy to produce nonlinear acoustic resonances in microscale SAW resonators or imaging acoustic black hole effects in wedges in the time domain.

References

1. T. Tachizaki, T. Muroya, O. Matsuda, Y. Sugawara, D. H. Hurley, and O. B. Wright: Rev. Sci. Inst. **77** (2006) 043713.
2. M. A. Mironov: Sov. Phys. Acoust. **34** (1988) 318.
3. V. V. Krylov and F.J.B.S. Tilman: J. Sound Vib. **274** (2004) 830.
4. C. Thomsen, H. T. Grahn, H. J. Maris, and J. Tauc: Phys. Rev. B **34** (1986) 4129.
5. R. E. Vines, M. R. Hauser, and J. P. Wolfe: Z. Phys. B **98** (1995) 255.